Supplementary Information for "Comparative Study of Folded/Unfolded Peptide Dynamics with Modern AMBER Force Fields and Water Models"

Michele Casoria,[†,‡] Marina Macchiagodena,[*,†] Anna Maria Papini,[‡,†] Claudia Andreini,[†,¶] Marco Pagliai,[*,†] and Piero Procacci[*,†]

†*Dipartimento di Chimica "Ugo Schiff", Università degli Studi di Firenze, Via della Lastruccia 3-13, I-50019 Sesto Fiorentino, Italy*

‡*Interdepartmental Research Unit of Peptide and Protein Chemistry and Biology, Università degli Studi di Firenze, Via della Lastruccia 13, I-50019 Sesto Fiorentino, Italy*

¶*Magnetic Resonance Center (CERM), Università degli Studi di Firenze, Via Luigi Sacconi 6, 50019 Sesto Fiorentino, Italy*

E-mail: marina.macchiagodena@unifi.it; marco.pagliai@unifi.it; piero.procacci@unifi.it

Force Fields Families

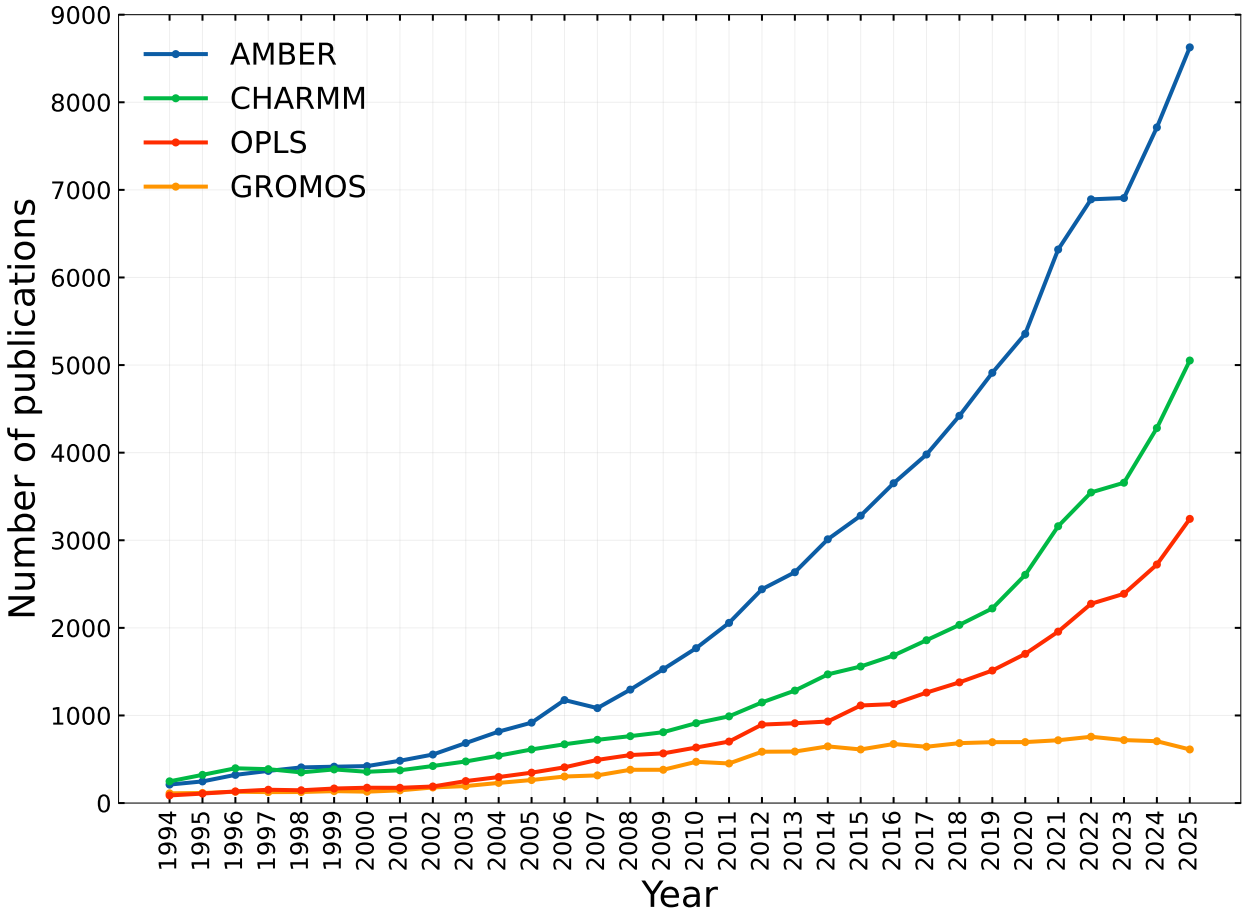

Figure S1: Documents published from 1994 to 2025 that reported the name of the FF family in one of the research fields. The analysis was conducted using Scopus on 6 February 2026.

AMBER Force Fields and Water Models

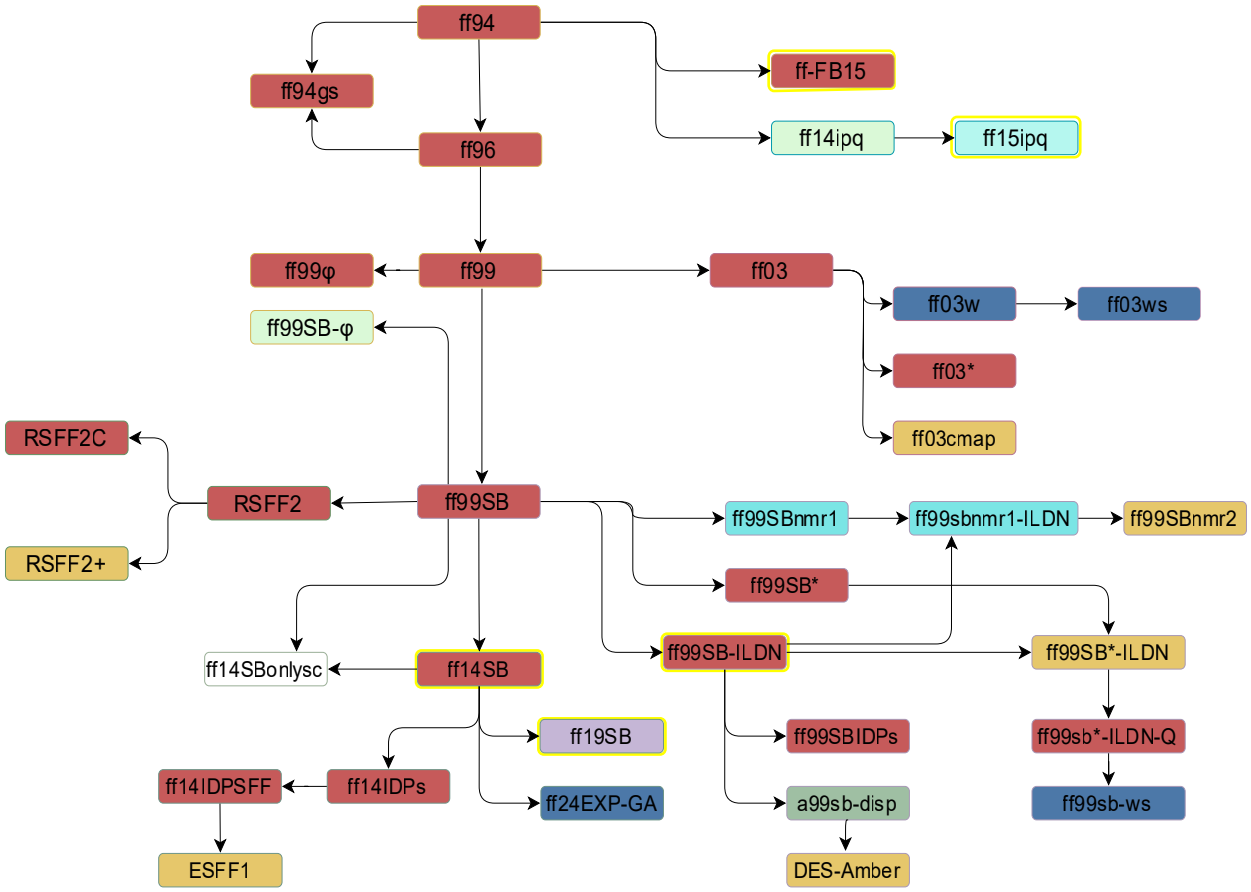

Figure S2: Schematic overview of force fields, highlighting with different colors the water model usually used to perform MD simulations: in red TIP3P,[1] in dark green TIP4P-Ew,[2] in light cyan SPC/E$_b$,[3] in blue TIP4P/2005,[4] in yellow TIP4P-D,[5] in dark cyan SPC/E,,[6] in light green a99SB-disp,[7] in violet OPC.[8] References for FFs: ff94,[9] ff96,[10] ff94gs,[11] ff-FB15,[12] ff14ipq,[13] ff15ipq,[14] ff99,[15] ff99ϕ,[16] ff03,[17] ff03w,[18] ff03*,[19] ff03cmap,[20] ff03ws,[21] ff99SB,[22] ff99SB-ϕ,[23] RSFF2,[24] RSFF2C,[25] RSFF2+,[26] ff99SBnmr1,,[27] ff99sbnmr1-ILDN,[27,28] ff99SBnmr2,[29] ff99SB*,[19] ff99SB-ILDN,[28] ff99SB*-ILDN,[19,28] ff99sb*-ILDN-Q,[30] ff99sb-ws,[21] ff99SBIDPs,[31] a99sb-disp,[7] DES-AMBER,[32] ff14SB,[33] ff19SB,[34] ff24EXP-GA,[35] ff14IDPs,[36] ff14IDPSFF,[37] ESFF1.[38]

Information for the Repository Navigation

The repository https://marinamacchiagodena.github.io/AMBERFFs-WaterModels/ contains the results of the analysis for all 95 FF-water model combinations. The following Figures

S3-S6 provide navigation information.

AMBERFFs-WaterModels

Comparative Study of Folded/Unfolded Peptide Dynamics with Modern AMBER Force Fields and Water Models

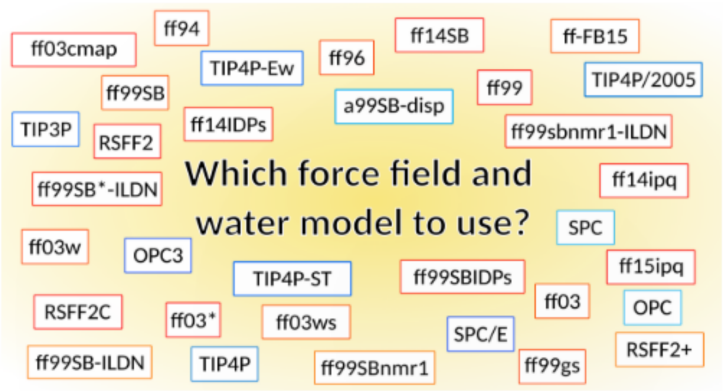

On this page we present the results of a comparative study in which 95 combinations of AMBER Force Fields and water models are used to simulate 4 different peptides performing Molecular Dynamics (MD) simulations. The four peptides have different secondary structures, and we verify which Force Field-Water Model combination better reproduces the experimental arrangment.

To visualize the results, it is necessary to select a **Peptide**, a **Force Field** and a **Water Model** HERE .

Details about the studied systems and the performed analysis can be found in this paper . The peptides studied have the following characteristics:

Peptide	PDB Code	Sequence	Motif	% Deposited	% Water
H1	1DJF	QAPAYKKAAKKLAES	α-helix	73%	5%
H2	1L2Y	NLYIQWLKDGGPSSGRPPPS	α-helix	35%	35%
B1	2GB1(2-19)	TYKLILNGKTLKGETTTE	ß-hairpin	55%	5%
B2	2GB1(41-56)	GEWTYDDATKTFTVTE	ß-hairpin	62%	25%

The five Force Fields tested are:

- ff99SB-ILDN , ff14SB , ff19SB , ff-FB15 , and ff15ipq with the nineteen Water Models:
  - SPC , TIP3P , SPC/E , TIP3P-Ew, SPC/Eb, TIP3P-FB, SPC/ϵ, OPC3, TIP3P-ST;
  - TIP4P, TIP4P-Ew, TIP4P/2005, TIP4P-FB , OPC, TIP4P/ϵ, TIP4P-D, a99SB-disp, TIP4P-ST, and TIP4P-BG.

Michele Casoria, Marina Macchiagodena, Anna Maria Papini, Claudia Andreini, Marco Pagliai,Piero Procacci
Dipartimento di Chimica "Ugo Schiff", Università degli Studi di Firenze, Via della Lastruccia 3, 50019 Sesto Fiorentino, Italy
If you have any questions, please feel free to contact the authors.

Figure S3: Main page. To choose the results, it is necessary to select the page indicated with an arrow.

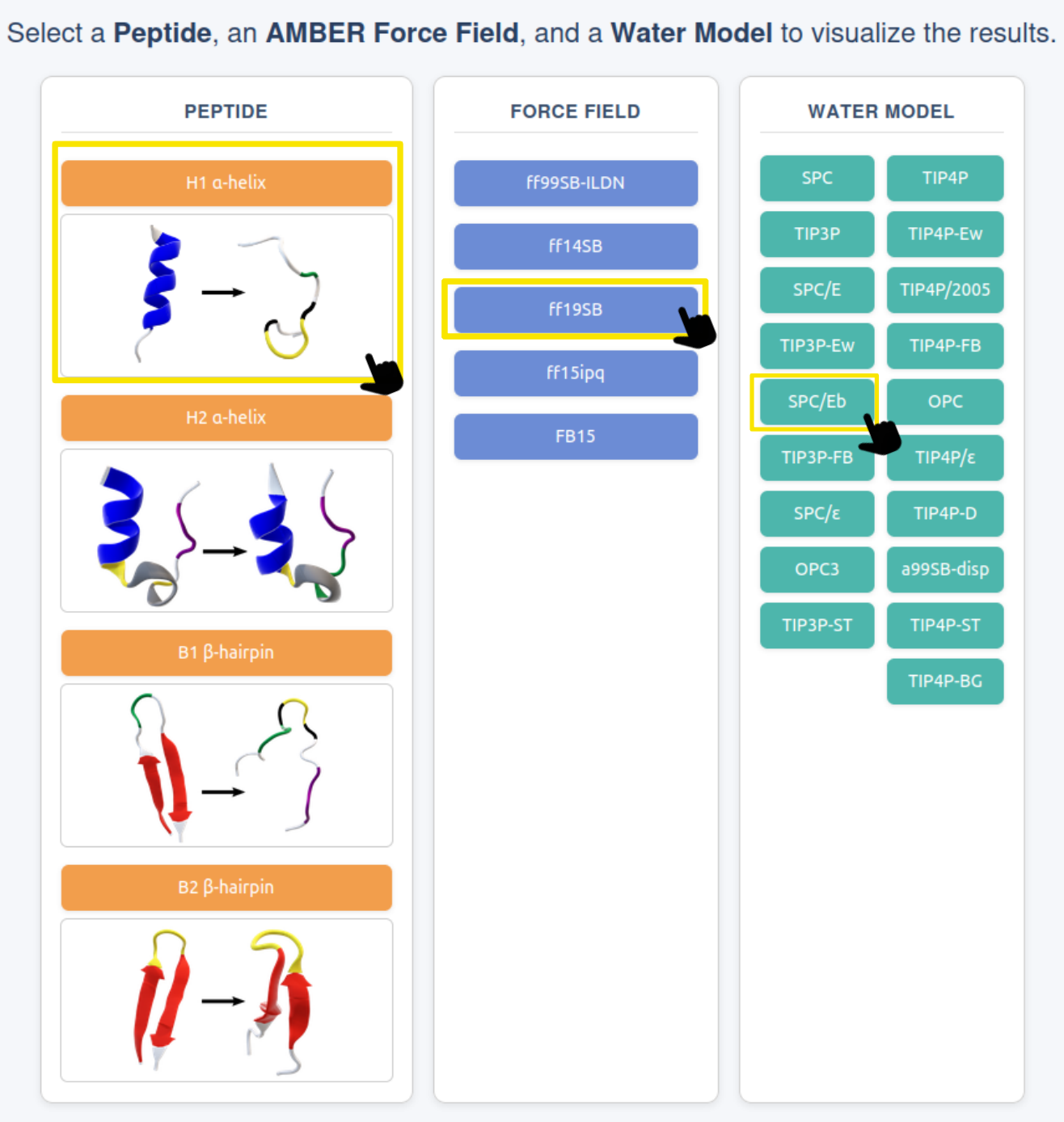

Figure S4: In this page, we can select the system and the FF-water model combination of interest.

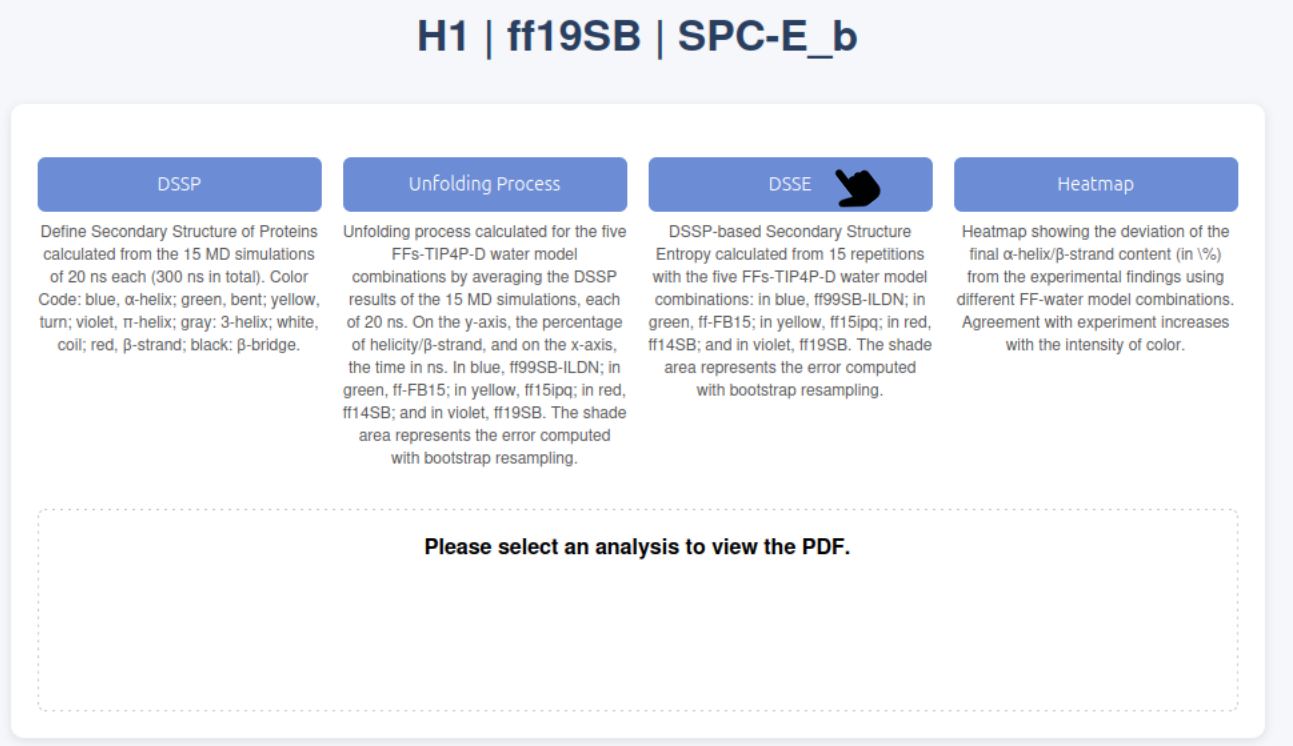

Figure S5: Once the triad system–FF–water model has been selected, a new page displaying the results is opened.

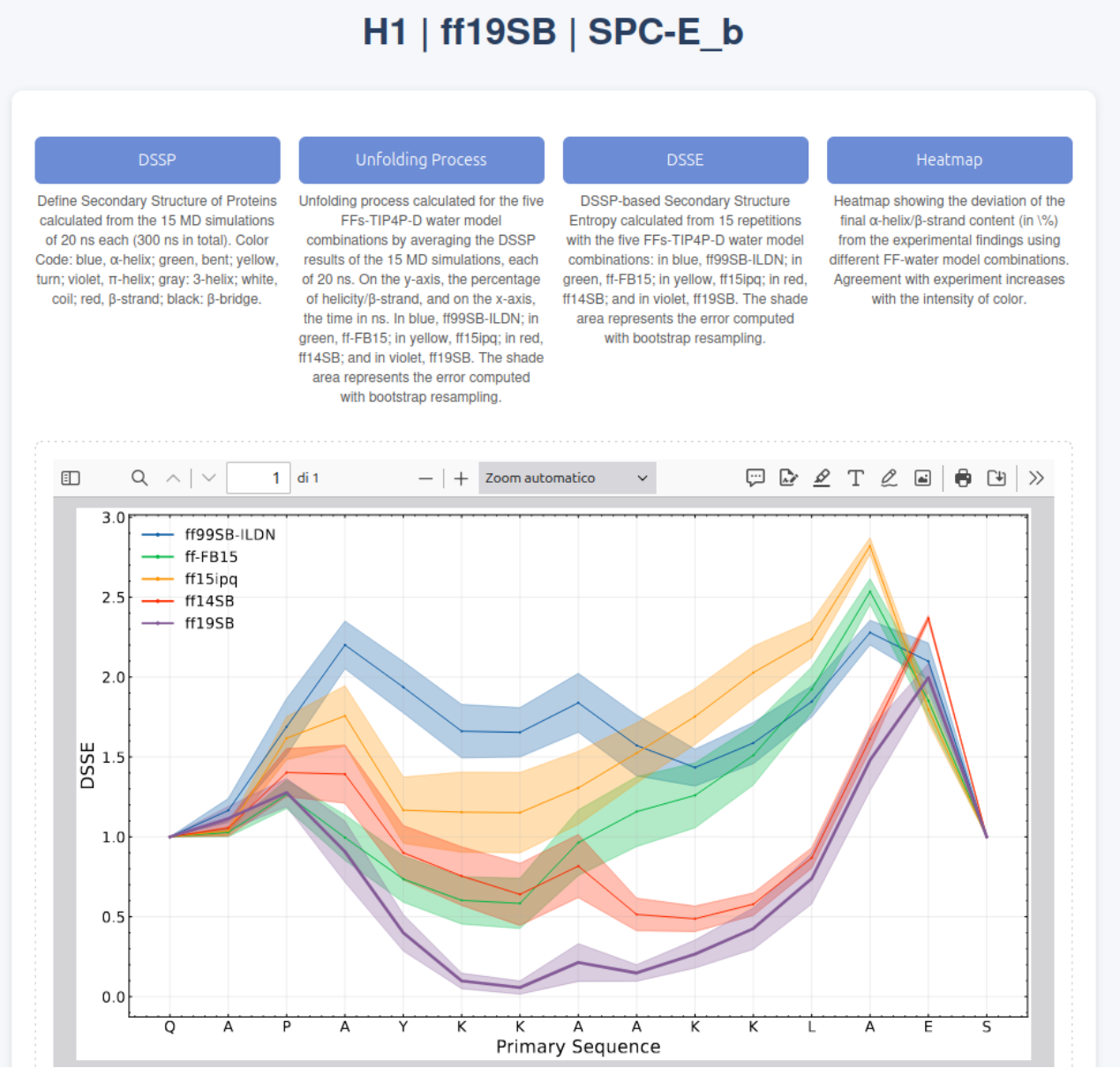

Figure S6: An example of the DSSE results for H1-ff19SB-SPC-E_b combination.

Secondary-structure Composition

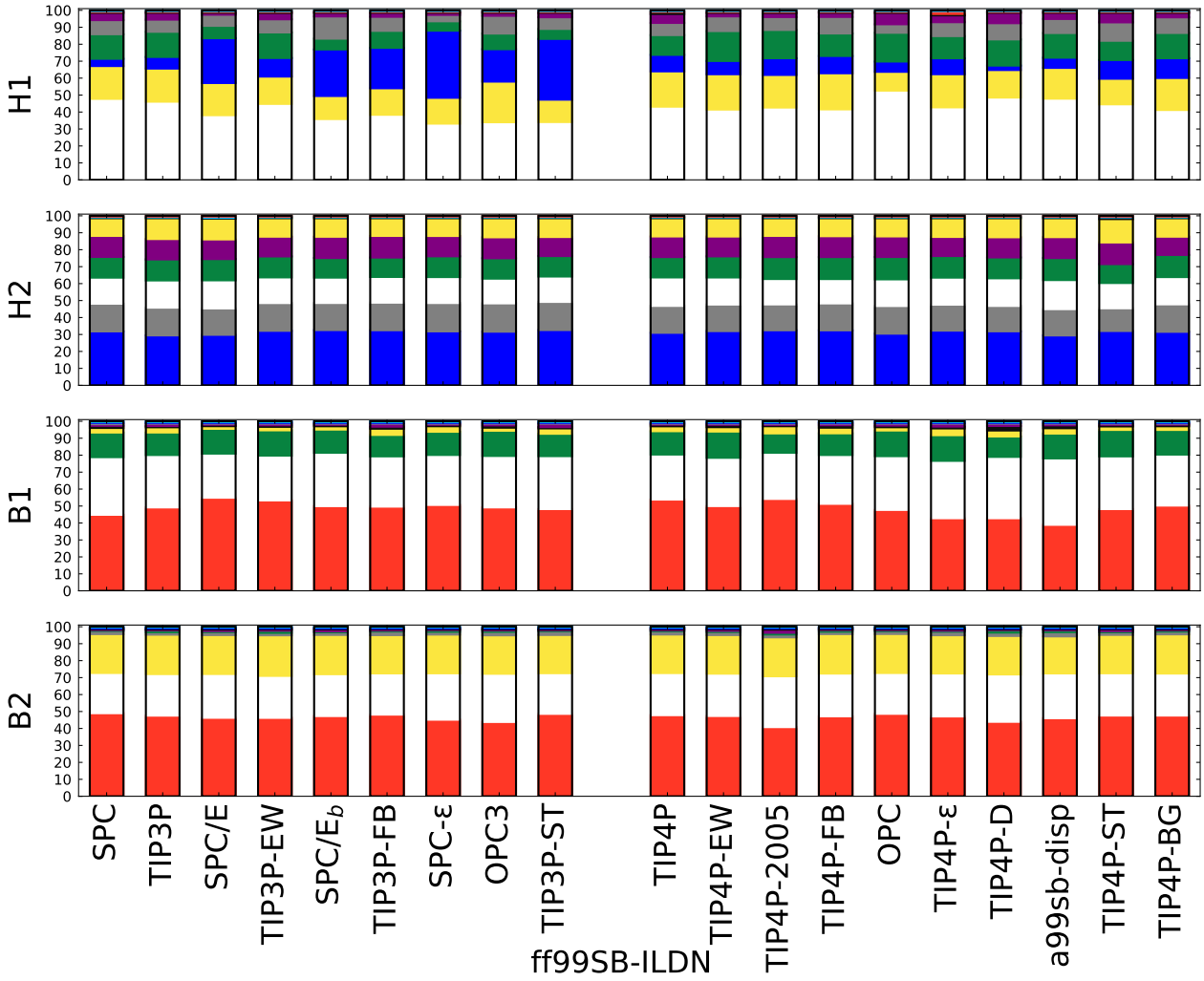

Figure S7: Secondary-structure composition of peptides H1, H2, B1, and B2 obtained from DSSP analysis at the final simulation time using the ff99SB-ILDN force field. Stacked bars report the percentage of residues assigned to each secondary-structure class (α-helix, 3_{10}-helix, π-helix, β-strand, β-bridge, turn, bend, and coil) across different water models. Values are averaged over 15 replicas and normalized to 100%. Color code: white, coil; red, β-strand; green, bend; yellow, turn; violet, π-helix; black, β-bridge.

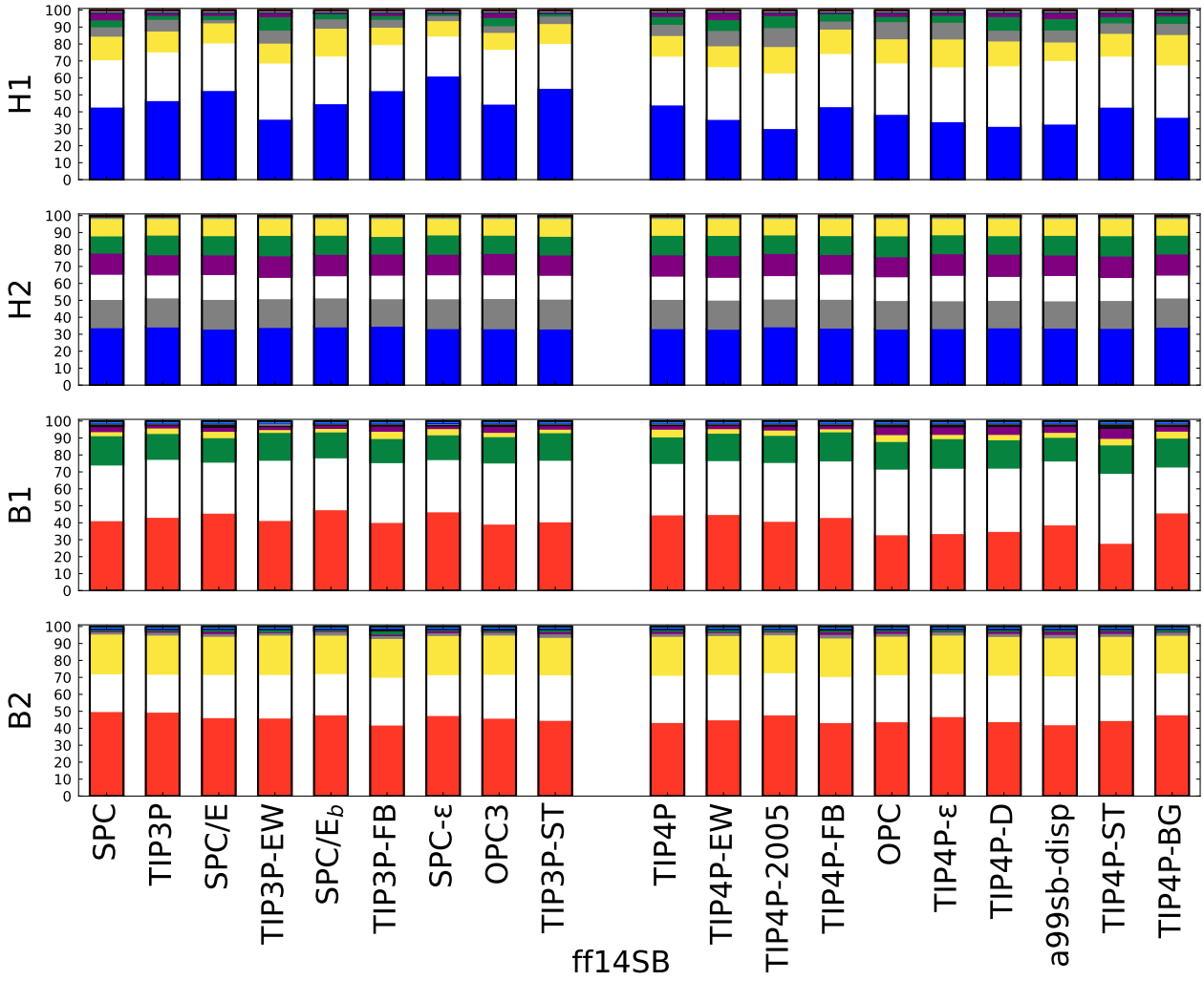

Figure S8: Secondary-structure composition of peptides H1, H2, B1, and B2 obtained from DSSP analysis at the final simulation time using the ff14SB force field. Stacked bars report the percentage of residues assigned to each secondary-structure class (α-helix, 3_{10}-helix, π-helix, β-strand, β-bridge, turn, bend, and coil) across different water models. Values are averaged over 15 replicas and normalized to 100%. Color code: white, coil; red, β-strand; green, bend; yellow, turn; violet, π-helix; black, β-bridge.

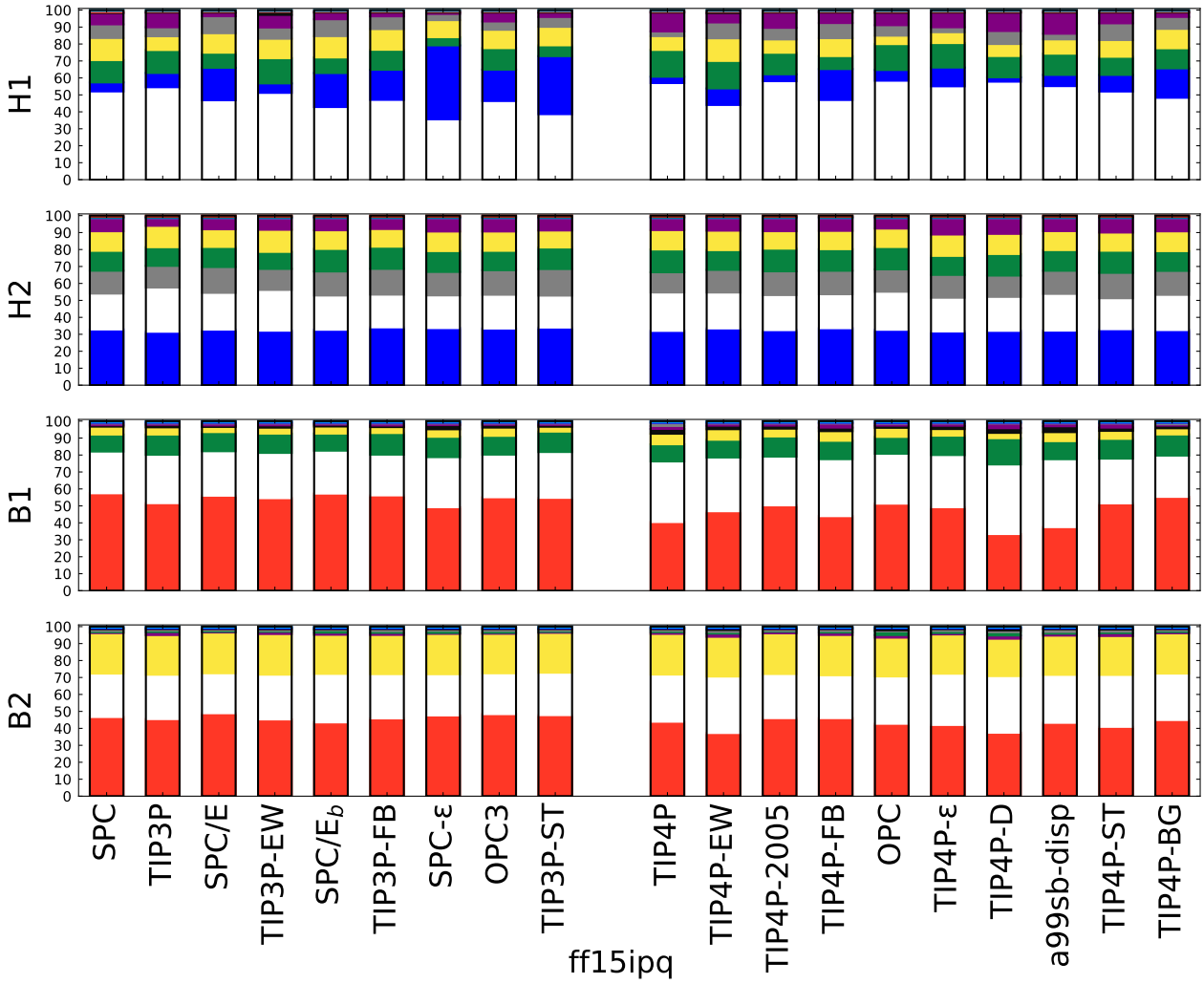

Figure S9: Secondary-structure composition of peptides H1, H2, B1, and B2 obtained from DSSP analysis at the final simulation time using the ff15ipq force field. Stacked bars report the percentage of residues assigned to each secondary-structure class (α-helix, 3_{10}-helix, π-helix, β-strand, β-bridge, turn, bend, and coil) across different water models. Values are averaged over 15 replicas and normalized to 100%. Color code: white, coil; red, β-strand; green, bend; yellow, turn; violet, π-helix; black, β-bridge.

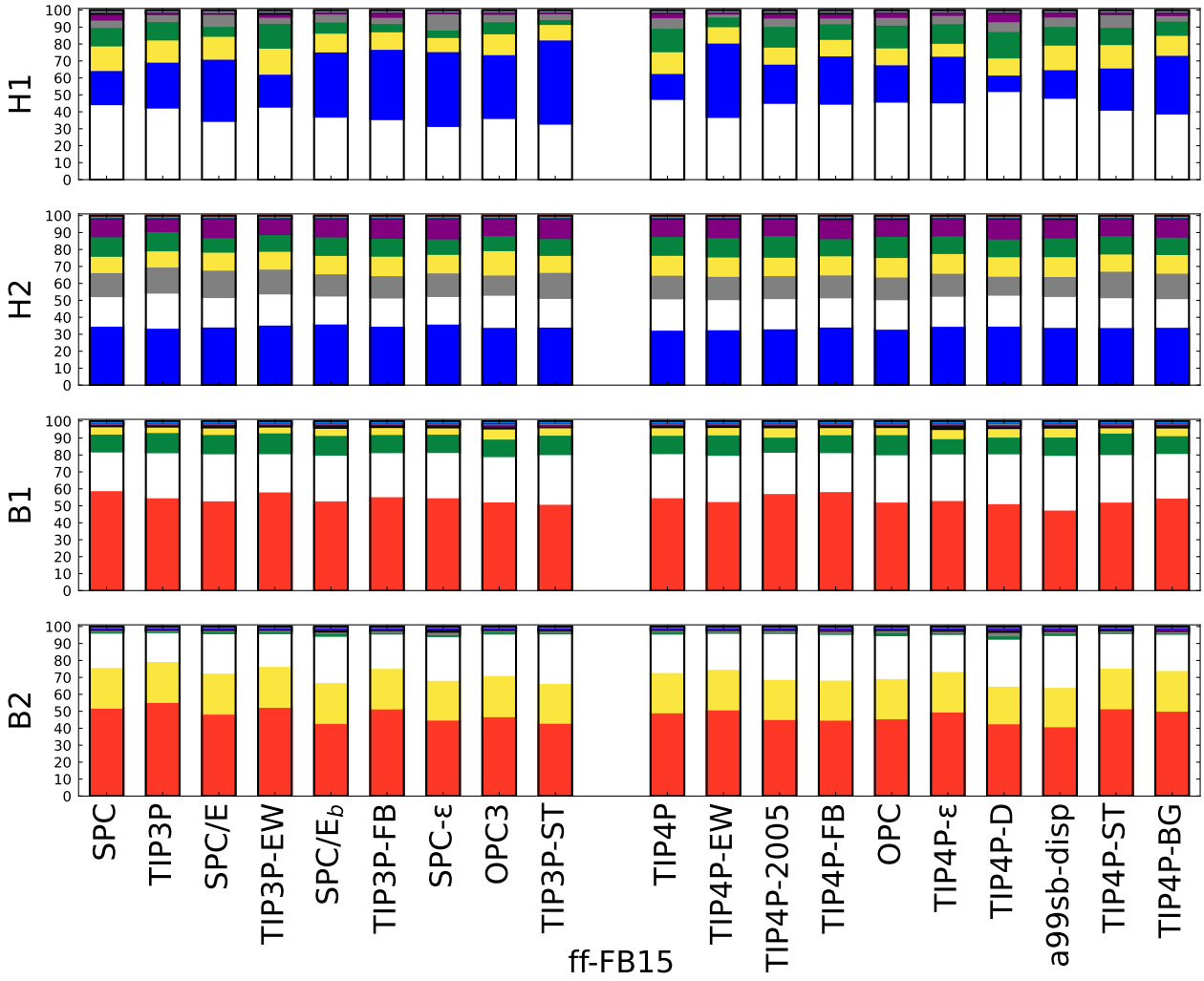

Figure S10: Secondary-structure composition of peptides H1, H2, B1, and B2 obtained from DSSP analysis at the final simulation time using the ff-FB15 force field. Stacked bars report the percentage of residues assigned to each secondary-structure class (α-helix, 3_{10}-helix, π-helix, β-strand, β-bridge, turn, bend, and coil) across different water models. Values are averaged over 15 replicas and normalized to 100%. Color code: white, coil; red, β-strand; green, bend; yellow, turn; violet, π-helix; black, β-bridge.

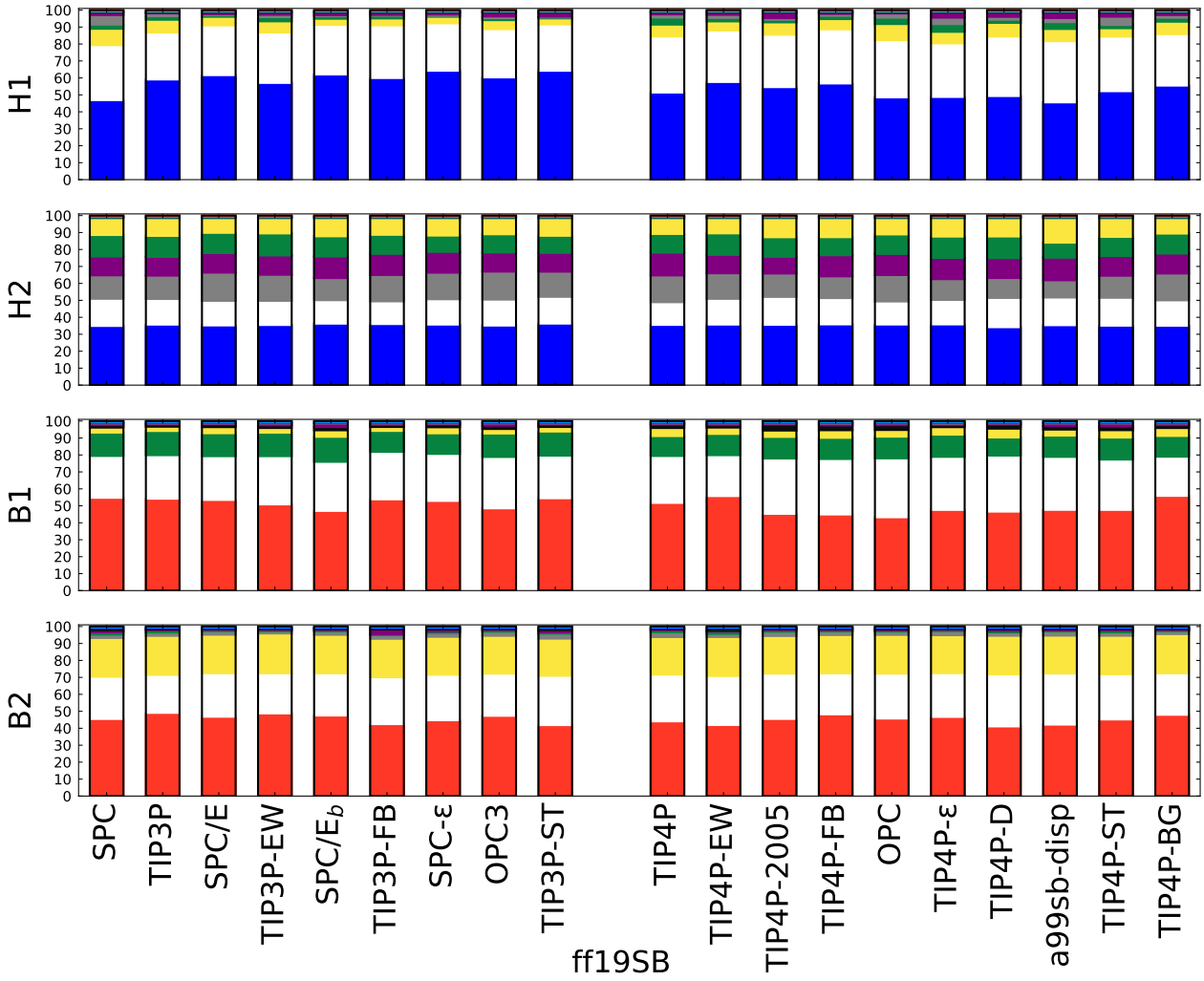

Figure S11: Secondary-structure composition of peptides H1, H2, B1, and B2 obtained from DSSP analysis at the final simulation time using the ff19SB force field. Stacked bars report the percentage of residues assigned to each secondary-structure class (α-helix, 3_{10}-helix, π-helix, β-strand, β-bridge, turn, bend, and coil) across different water models. Values are averaged over 15 replicas and normalized to 100%. Color code: white, coil; red, β-strand; green, bend; yellow, turn; violet, π-helix; black, β-bridge.

Analysis for B1 and B2 at Higher Temperature (340 K)

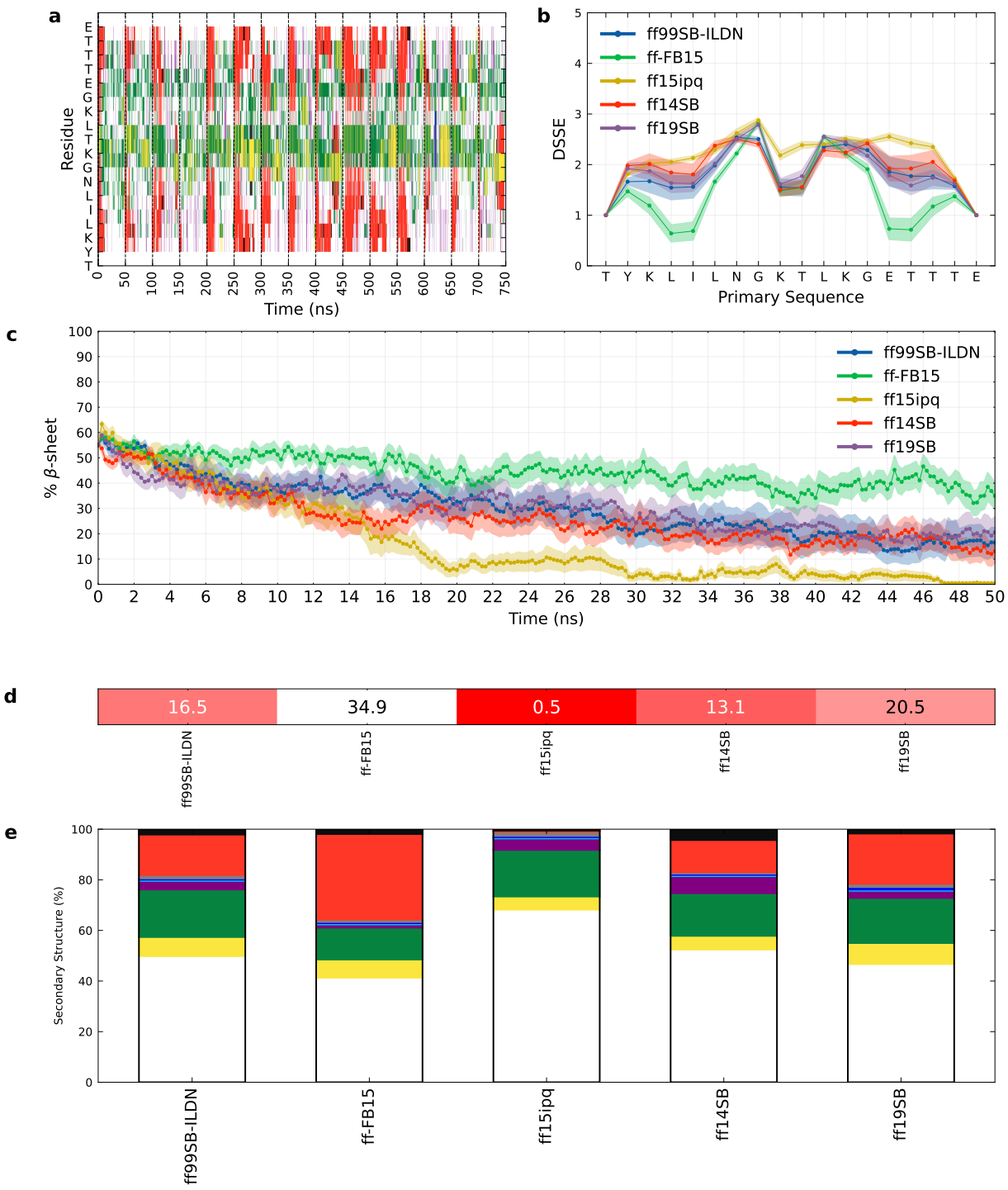

Figure S12: **a**: B1 DSSP calculated from 15 MD simulations of 50 ns each (750 ns in total), with ff15ipq-TIP4P-D water model combination. Color Code: white, coil; red, β-strand; green, bent; yellow, turn; violet, π-helix; black: β-bridge. (Caption continues on next page.)

Figure S12: (Continued) **b**: B1 DSSE calculated from the 15 MD with the five FFs-TIP4P-D water model combinations: in blue, ff99SB-ILDN; in green, ff-FB15; in yellow, ff15ipq; in red, ff14SB; and in violet, ff19SB. The shaded area represents the error computed with bootstrap resampling. **c**: B1 unfolding process calculated for the five FFs-TIP4P-D water model combinations by averaging the DSSP results of the 15 MD simulations. On the y-axis, the percentage of β-sheet, and on the x-axis, the time in ns. In blue, ff99SB-ILDN; in green, ff-FB15; in yellow, ff15ipq; in red, ff14SB; and in violet, ff19SB. The shaded area represents the error computed with bootstrap resampling. **d**: B1 heatmap showing the deviation of the final β-sheet content (in %) from the experimental findings. Agreement with the experiment increases with the intensity of the red color. **e**: Secondary-structure composition of peptide B1 obtained from DSSP analysis at the final simulation time using all FFs combined with TIP4P-D water model. Stacked bars report the percentage of residues assigned to each secondary-structure class (α-helix, 310-helix, π-helix, β-strand, β-bridge, turn, bend, and coil) across different water models. Values are averaged over 15 replicas and normalized to 100%. Color code: white, coil; red, β-strand; green, bend; yellow, turn; violet, π-helix; black, β-bridge, blue, α-helix; gray: 3-helix.

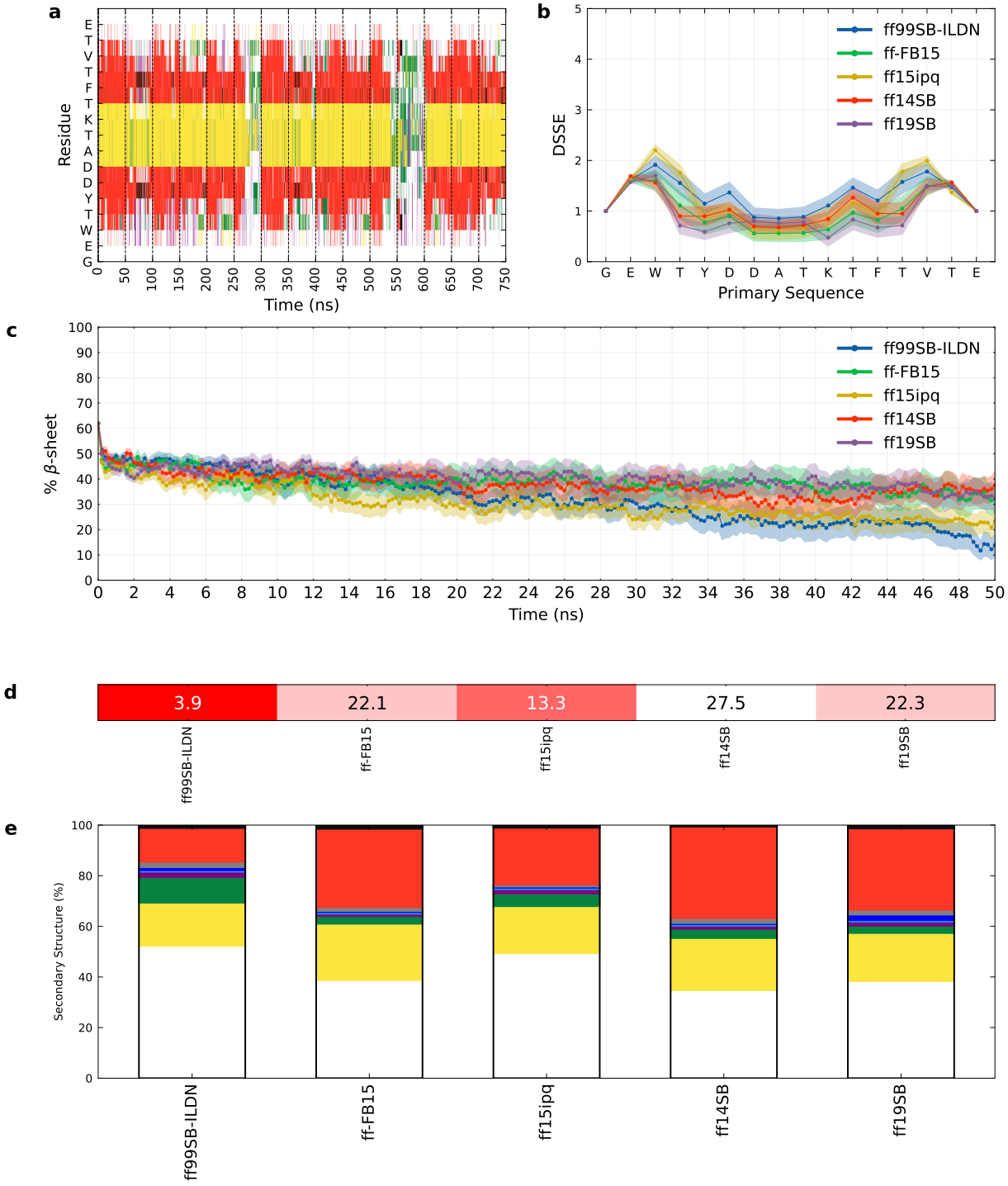

Figure S13: **a**: B2 DSSP calculated from 15 MD simulations of 50 ns each (750 ns in total), with ff15ipq-TIP4P-D water model combination. Color Code: white, coil; red, β-strand; green, bent; yellow, turn; violet, π-helix; black: β-bridge. (Caption continues on next page.)

Figure S13: (Continued) **b**: B2 DSSE calculated from the 15 MD with the five FFs-TIP4P-D water model combinations: in blue, ff99SB-ILDN; in green, ff-FB15; in yellow, ff15ipq; in red, ff14SB; and in violet, ff19SB. The shaded area represents the error computed with bootstrap resampling. **c**: B2 unfolding process calculated for the five FFs-TIP4P-D water model combinations by averaging the DSSP results of the 15 MD simulations. On the y-axis, the percentage of β-sheet, and on the x-axis, the time in ns. In blue, ff99SB-ILDN; in green, ff-FB15; in yellow, ff15ipq; in red, ff14SB; and in violet, ff19SB. The shaded area represents the error computed with bootstrap resampling. **d**: B2 heatmap showing the deviation of the final β-sheet content (in %) from the experimental findings. Agreement with the experiment increases with the intensity of the red color. **e**: Secondary-structure composition of peptide B2 obtained from DSSP analysis at the final simulation time using all FFs combined with TIP4P-D water model. Stacked bars report the percentage of residues assigned to each secondary-structure class (α-helix, 310-helix, π-helix, β-strand, β-bridge, turn, bend, and coil) across different water models. Values are averaged over 15 replicas and normalized to 100%. Color code: white, coil; red, β-strand; green, bend; yellow, turn; violet, π-helix; black, β-bridge, blue, α-helix; gray: 3-helix.

Water Models

Table S1: Parameters of the 3-site water models used in the present benchmark. All values are rounded to the same number of decimal places.

Model	Year	d_{OH} [Å]	θ_{OH} [°]	q_O [e]	σ_O [nm]	ε_O [kJ/mol]
SPC[39]	1981	1.0000	109.47	-0.82000	0.31660	0.65000
TIP3P[1]	1983	0.9572	104.52	-0.83400	0.31508	0.63639
SPC/E[6]	1987	1.0000	109.47	-0.84760	0.31660	0.65000
TIP3P-Ew[40]	2004	0.9572	104.52	-0.83000	0.31880	0.42677
SPC/E_b[3]	2012	1.0100	109.47	-0.84760	0.31658	0.64978
TIP3P-FB[41]	2014	1.0118	108.15	-0.84844	0.31780	0.65214
SPC/ε[42]	2015	1.0000	109.45	-0.89000	0.31785	0.70586
OPC3[43]	2016	0.9789	109.47	-0.89517	0.31743	0.68370
TIP3P-ST[44]	2019	1.0230	108.11	-0.85112	0.31926	0.60191

Table S2: Parameters of the 4-site water models used in the present benchmark. All values are rounded to the same number of decimal places.

Model	Year	d_{OH} [Å]	θ_{OH} [°]	q_M [e]	d_{MO} [Å]	σ_O [nm]	ε_O [kJ/mol]
TIP4P[1]	1983	0.9572	104.52	-1.04000	0.15000	0.31536	0.64852
TIP4P-Ew[2]	2004	0.9572	104.52	-1.04844	0.12500	0.31644	0.68095
TIP4P/2005[4]	2005	0.9572	104.52	-1.11280	0.15460	0.31589	0.77490
TIP4P-FB[41]	2014	0.9572	104.52	-1.05174	0.10527	0.31656	0.74928
OPC[8]	2014	0.8724	103.60	-1.35828	0.15940	0.31666	0.89036
TIP4P/ε[45]	2014	0.9572	104.52	-1.05400	0.10500	0.31650	0.77325
TIP4P-D[5]	2015	0.9572	104.52	-1.16000	0.15460	0.31650	0.93655
a99SB-disp[7]	2018	0.9572	104.52	-1.18000	0.15460	0.31650	0.99899
TIP4P-ST[44]	2019	0.9572	108.11	-1.04344	0.09890	0.31661	0.74030
TIP4P-BG[46]	2021	0.9572	104.52	-1.02488	0.12097	0.31640	0.59966

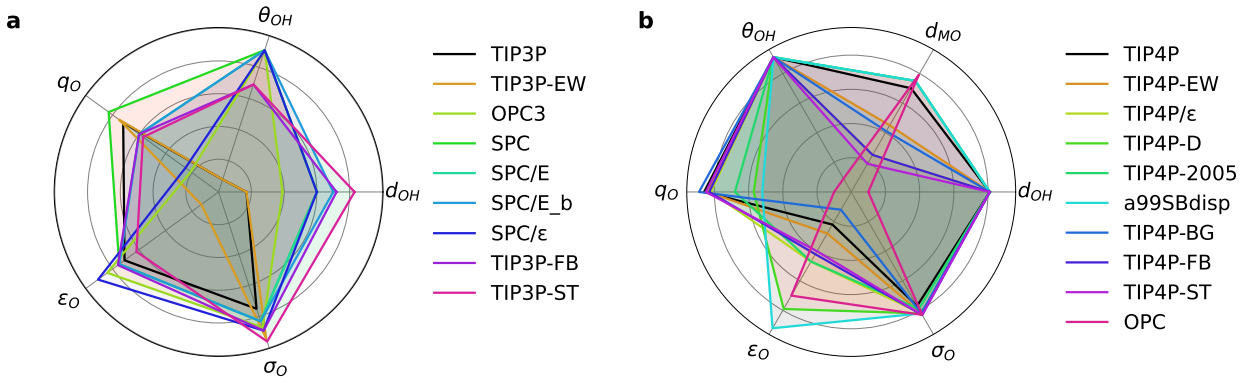

Figure S14: Radar plot comparison of geometric and electrostatic parameters for three-site (left) and four-site (right) water models. Values are normalized with respect to the min–max range of each parameter within the respective group. Parameter ranges: $d_{OH} \in [0.86, 0.98]$ Å, $\theta_{OH} \in [103.5, 104.62]^\circ$, $q_O \in [-1.40, -0.98]$ e, $\sigma_O \in [0.30, 0.32]$ nm, $\varepsilon_O \in [0.54, 1.04]$ kJ/mol, $d_{MO} \in [0.08, 0.18]$ Å.

Multivariate Linear Regression Analysis

Table S3: Multivariate linear regression results for 3-site water models. The dependent variable is defined as the deviation from the average secondary-structure stability of peptides H1 and B1. Predictors (dipole μ, LJ σ, LJ ϵ) were standardized before fitting. Reported are average value ($\overline{x}$), standard deviation (σ_x), regression coefficients (β), standard errors ($\mathrm{SE}_{\overline{x}}$), and statistical significance (p-values).

Parameter	$\overline{x}$	σ_x	β	$\mathrm{SE}_{\overline{x}}$	p-value
μ	2.434	0.130	6.049	1.731	<0.001
σ	0.317	0.001	0.608	0.513	0.236
ϵ	0.708	0.127	2.162	1.069	0.043

Table S4: Multivariate linear regression results for 4-site water models. The dependent variable is defined as the deviation from the average secondary-structure stability of peptides H1 and B1. Predictors (dipole μ, LJ σ, LJ ϵ) were standardized before fitting. Reported are average value ($\overline{x}$), standard deviation (σ_x), regression coefficients (β), standard errors ($\mathrm{SE}_{\overline{x}}$), and statistical significance (p-values).

Parameter	$\overline{x}$	σ_x	β	$\mathrm{SE}_{\overline{x}}$	p-value
μ	2.434	0.130	0.263	0.338	0.437
σ	0.317	0.001	2.242	1.277	0.079
ϵ	0.708	0.127	-3.826	0.595	<0.001

References

(1) Jorgensen, W. L.; Chandrasekhar, J.; Madura, J. D.; Impey, R. W.; Klein, M. L. Comparison of simple potential functions for simulating liquid water. *J. Chem. Phys.* **1983**, *79*, 926–935.

(2) Vega, C.; Abascal, J. L. F.; Nezbeda, I. Vapor-liquid equilibria from the triple point up to the critical point for the new generation of TIP4P-like models: TIP4P/Ew, TIP4P/2005, and TIP4P/ice. *J. Chem. Phys.* **2006**, *125*, 034503.

(3) Takemura, K.; Kitao, A. Water Model Tuning for Improved Reproduction of Rotational Diffusion and NMR Spectral Density. *J. Phys. Chem. B.* **2012**, *116*, 6279–6287.

(4) Abascal, J. L. F.; Vega, C. A general purpose model for the condensed phases of water: TIP4P/2005. *J. Chem. Phys.* **2005**, *123*, 234505.

(5) Piana, S.; Donchev, A. G.; Robustelli, P.; Shaw, D. E. Water Dispersion Interactions Strongly Influence Simulated Structural Properties of Disordered Protein States. *J. Phys. Chem. B.* **2015**, *119*, 5113–5123.

(6) Berendsen, H. J. C.; Grigera, J. R.; Straatsma, T. P. The Missing Term in Effective Pair Potentials. *J. Phys. Chem.* **1987**, *91*, 6269–6271.

(7) Robustelli, P.; Piana, S.; Shaw, D. E. Developing a molecular dynamics force field for both folded and disordered protein states. *Proc. Natl. Acad. Sci. U.S.A.* **2018**, *115*, E4758 – E4766.

(8) Izadi, S.; Anandakrishnan, R.; Onufriev, A. V. Building Water Models: A Different Approach. *J. Phys. Chem. Lett.* **2014**, *5*, 3863–3871.

(9) Cornell, W. D.; Cieplak, P.; Bayly, C. I.; Gould, I. R.; Merz, K. M.; Ferguson, D. M.; Spellmeyer, D. C.; Fox, T.; Caldwell, J. W.; Kollman, P. A. A Second Generation

Force Field for the Simulation of Proteins, Nucleic Acids, and Organic Molecules. *J. Am. Chem. Soc.* **1995**, *117*, 5179–5197.

(10) Kollman, P.; Dixon, R.; Cornell, W.; Fox, T.; Chipot, C.; Pohorille, A. In *Computer Simulation of Biomolecular Systems: Theoretical and Experimental Applications*; van Gunsteren, W. F., Weiner, P. K., Wilkinson, A. J., Eds.; Springer Netherlands: Dordrecht, 1997; pp 83–96.

(11) García, A. E.; Sanbonmatsu, K. Y. α-Helical stabilization by side chain shielding of backbone hydrogen bonds. *Proc. Natl. Acad. Sci. U.S.A.* **2002**, *99*, 2782–2787.

(12) Wang, L.-P.; McKiernan, K. A.; Gomes, J.; Beauchamp, K. A.; Head-Gordon, T.; Rice, J. E.; Swope, W. C.; Martínez, T. J.; Pande, V. S. Building a More Predictive Protein Force Field: A Systematic and Reproducible Route to AMBER-FB15. *J. Phys. Chem. B.* **2017**, *121*, 4023–4039.

(13) Cerutti, D. S.; Swope, W. C.; Rice, J. E.; Case, D. A. ff14ipq: A Self-Consistent Force Field for Condensed-Phase Simulations of Proteins. *J. Chem. Theory Comput.* **2014**, *10*, 4515–4534.

(14) Debiec, K. T.; Cerutti, D. S.; Baker, L. R.; Gronenborn, A. M.; Case, D. A.; Chong, L. T. Further along the Road Less Traveled: AMBER ff15ipq, an Original Protein Force Field Built on a Self-Consistent Physical Model. *J. Chem. Theory Comput.* **2016**, *12*, 3926–3947.

(15) Wang, J.; Cieplak, P.; Kollman, P. A. How well does a restrained electrostatic potential (RESP) model perform in calculating conformational energies of organic and biological molecules? *J. Comput. Chem.* **2000**, *21*, 1049–1074.

(16) Sorin, E. J.; Pande, V. S. Exploring the Helix-Coil Transition via All-Atom Equilibrium Ensemble Simulations. *Biophys. J.* **2005**, *88*, 2472–2493.

(17) Duan, Y.; Wu, C.; Chowdhury, S.; Lee, M. C.; Xiong, G.; Zhang, W.; Yang, R.; Cieplak, P.; Luo, R.; Lee, T.; Caldwell, J.; Wang, J.; Kollman, P. A point-charge force field for molecular mechanics simulations of proteins based on condensed-phase quantum mechanical calculations. *J. Comput. Chem.* **2003**, *24*, 1999–2012.

(18) Best, R. B.; Mittal, J. Protein Simulations with an Optimized Water Model: Cooperative Helix Formation and Temperature-Induced Unfolded State Collapse. *J. Phys. Chem. B.* **2010**, *114*, 14916–14923.

(19) Best, R. B.; Hummer, G. Optimized Molecular Dynamics Force Fields Applied to the Helix Coil Transition of Polypeptides. *J. Phys. Chem. B.* **2009**, *113*, 9004–9015.

(20) Zhang, Y.; Liu, H.; Yang, S.; Luo, R.; Chen, H.-F. Well-Balanced Force Field ff03CMAP for Folded and Disordered Proteins. *J. Chem. Theory Comput.* **2019**, *15*, 6769–6780.

(21) Best, R. B.; Zheng, W.; Mittal, J. Balanced Protein–Water Interactions Improve Properties of Disordered Proteins and Non-Specific Protein Association. *J. Chem. Theory Comput.* **2014**, *10*, 5113–5124.

(22) Hornak, V.; Abel, R.; Okur, A.; Strockbine, B.; Roitberg, A.; Simmerling, C. Comparison of multiple Amber force fields and development of improved protein backbone parameters. *Proteins: Struct., Funct., Bioinf.* **2006**, *65*, 712–725.

(23) Nerenberg, P. S.; Head-Gordon, T. Optimizing Protein Solvent Force Fields to Reproduce Intrinsic Conformational Preferences of Model Peptides. *J. Chem. Theory Comput.* **2011**, *7*, 1220–1230.

(24) Zhou, C.-Y.; Jiang, F.; Wu, Y.-D. Residue-Specific Force Field Based on Protein Coil Library. RSFF2: Modification of AMBER ff99SB. *J. Phys. Chem. B.* **2015**, *119*, 1035–1047.

(25) Kang, W.; Jiang, F.; Wu, Y.-D. Universal Implementation of a Residue-Specific Force Field Based on CMAP Potentials and Free Energy Decomposition. *J. Chem. Theory Comput.* **2018**, *14*, 4474–4486.

(26) Wu, H.-N.; Jiang, F.; Wu, Y.-D. Significantly Improved Protein Folding Thermodynamics Using a Dispersion-Corrected Water Model and a New Residue-Specific Force Field. *J. Phys. Chem. Lett.* **2017**, *8*, 3199–3205.

(27) Li, D.-W.; Brüschweiler, R. NMR-Based Protein Potentials. *Angew. Chem. Int. Ed.* **2010**, *49*, 6778–6780.

(28) Lindorff-Larsen, K.; Piana, S.; Palmo, K.; Maragakis, P.; Klepeis, J. L.; Dror, R. O.; Shaw, D. E. Improved side-chain torsion potentials for the Amber ff99SB protein force field. *Proteins: Struct., Funct., Bioinf.* **2010**, *78*, 1950–1958.

(29) Yu, L.; Li, D.-W.; Brüschweiler, R. Balanced Amino-Acid-Specific Molecular Dynamics Force Field for the Realistic Simulation of Both Folded and Disordered Proteins. *J. Chem. Theory Comput.* **2020**, *16*, 1311–1318.

(30) Best, R. B.; de Sancho, D.; Mittal, J. Residue-specific α-helix propensities from molecular simulation. *Biophys. J.* **2012**, *102*, 1462–1467.

(31) Wang, W.; Ye, W.; Jiang, C.; Luo, R.; Chen, H.-F. New Force Field on Modeling Intrinsically Disordered Proteins. *Chem. Biol. Drug Des.* **2014**, *84*, 253–269.

(32) Piana, S.; Robustelli, P.; Tan, D.; Chen, S.; Shaw, D. E. Development of a Force Field for the Simulation of Single-Chain Proteins and Protein–Protein Complexes. *J. Chem. Theory Comput.* **2020**, *16*, 2494–2507.

(33) Maier, J. A.; Martinez, C.; Kasavajhala, K.; Wickstrom, L.; Hauser, K. E.; Simmerling, C. ff14SB: Improving the Accuracy of Protein Side Chain and Backbone Parameters from ff99SB. *J. Chem. Theory Comput.* **2015**, *11*, 3696–3713.

(34) Tian, C.; Kasavajhala, K.; Belfon, K. A. A.; Raguette, L.; Huang, H.; Migues, A. N.; Bickel, J.; Wang, Y.; Pincay, J.; Wu, Q.; Simmerling, C. ff19SB: Amino-Acid-Specific Protein Backbone Parameters Trained against Quantum Mechanics Energy Surfaces in Solution. *J. Chem. Theory Comput.* **2020**, *16*, 528–552.

(35) Suresh, A.; Schweitzer-Stenner, R.; Urbanc, B. Amber ff24EXP-GA, Based on Empirical Ramachandran Distributions of Glycine and Alanine Residues in Water. *J. Chem. Theory Comput.* **2025**, *21*, 2515–2534.

(36) Song, D.; Wang, W.; Ye, W.; Ji, D.; Luo, R.; Chen, H.-F. ff14IDPs force field improving the conformation sampling of intrinsically disordered proteins. *Chem. Biol. Drug Des.* **2017**, *89*, 5–15.

(37) Song, D.; Luo, R.; Chen, H.-F. The IDP-Specific Force Field ff14IDPSFF Improves the Conformer Sampling of Intrinsically Disordered Proteins. *J. Chem. Inf. Model.* **2017**, *57*, 1166–1178.

(38) Song, D.; Liu, H.; Luo, R.; Chen, H.-F. Environment-Specific Force Field for Intrinsically Disordered and Ordered Proteins. *J. Chem. Inf. Model.* **2020**, *60*, 2257–2267.

(39) Berendsen, H. J. C.; Postma, J. P. M.; van Gunsteren, W. F.; Hermans, J. In *Intermolecular Forces: Proceedings of the Fourteenth Jerusalem Symposium on Quantum Chemistry and Biochemistry Held in Jerusalem, Israel, April 13–16, 1981*; Pullman, B., Ed.; Springer Netherlands: Dordrecht, 1981; pp 331–342.

(40) Price, D. J.; Brooks, I., Charles L. A modified TIP3P water potential for simulation with Ewald summation. *J. Chem. Phys.* **2004**, *121*, 10096–10103.

(41) Wang, L.-P.; Martinez, T. J.; Pande, V. S. Building Force Fields: An Automatic, Systematic, and Reproducible Approach. *J. Phys. Chem. Lett.* **2014**, *5*, 1885–1891.

(42) Fuentes-Azcatl, R.; Mendoza, N.; Alejandre, J. Improved SPC force field of water based on the dielectric constant: SPC/ϵ. *Phys. A: Stat. Mech. Appl.* **2015**, *420*, 116–123.

(43) Izadi, S.; Onufriev, A. V. Accuracy Limit of Rigid 3-Point Water Models. *J. Chem. Phys* **2016**, *145*, 074501.

(44) Qiu, Y.; Nerenberg, P. S.; Head-Gordon, T.; Wang, L.-P. Systematic Optimization of Water Models Using Liquid/Vapor Surface Tension Data. *J. Phys. Chem. B.* **2019**, *123*, 7061–7073.

(45) Fuentes-Azcatl, R.; Alejandre, J. Non-Polarizable Force Field of Water Based on the Dielectric Constant: TIP4P/ϵ. *J. Phys. Chem. B.* **2014**, *118*, 1263–1272.

(46) Ye, H.-f.; Wang, J.; Zheng, Y.-g.; Zhang, H.-w.; Chen, Z. Machine learning for reparameterization of four-site water models: TIP4P-BG and TIP4P-BGT. *Phys. Chem. Chem. Phys.* **2021**, *23*, 10164–10173.